

NATIONAL INSTITUTE FOR FUSION SCIENCE**Effect of Weak Dissipation on a Drift Orbit Mapping**

T. Yamagishi

(Received - Mar. 2, 2000)

NIFS-629

Mar. 2000

This report was prepared as a preprint of work performed as a collaboration research of the National Institute for Fusion Science (NIFS) of Japan. This document is intended for information only and for future publication in a journal after some rearrangements of its contents.

Inquiries about copyright and reproduction should be addressed to the Research Information Center, National Institute for Fusion Science, Oroshi-cho, Toki-shi, Gifu-ken 509-02 Japan.

RESEARCH REPORT
NIFS Series

Effect of Weak Dissipation on a Drift Orbit Mapping

Tomejiro Yamagishi

Tokyo Metropolitan Institute of Technology

Abstract

The effect of weak dissipation on drift orbits has been investigated making use of a simple mapping model in a helical magnetic field. It is found that, after many mapping iterations, any orbit tends to an attractor forming a vortex line even with very small dissipation. The convergence is faster for larger dissipation, i.e., the number of iteration N to converge within a certain distance from the attractor is inversely proportional to the amount of the dissipation. Although the behavior of orbits completely change, the basic stability characteristics of the system does not change, i.e., the coordinate of the attractors are determined by the stable fixed points in the area preserving system because the dissipation is very small. Since wide range of orbits are concentrated around the attractors after many toroidal circulations, a pinch effect is created by a small dissipation. Application of this pinch effect to fusion plasmas is discussed.

Keywords: drift orbit mapping for electron, weak dissipation, attractor, basin, nonlinear initial value problem, concentration of plasma, pinch effect.

§ 1. Introduction

Trajectory of a charged particle in an electromagnetic field has usually been investigated in the area preserving or Hamiltonian system. In any actual physical systems, however, there must be a certain dissipation which may be very small in some cases. The conservative system and the dissipative system are, however, entirely different worlds, and therefore, they are studied in entirely different manners. The behavior of trajectories are also different: A regular trajectory in a conservative system forms "surface" around a stable fixed point. When the trajectory becomes unstable or chaotic, the Poincare mapping of the trajectory becomes ergodic or fill uniformly in certain area. While in a dissipative system, a regular trajectory converges to an

attractor. In the chaotic state, it converges to the strange attractor.

No matter how small the dissipation is, if it is introduced in a Hamiltonian system, the trajectories should converge to attractors in the dissipative system. The purpose of the present paper, therefore, is to investigate how the orbits in the Hamiltonian system may change and tend to attractors in the dissipative system when a small dissipation is introduced. To investigate the convergence of orbits to attractors, we will employ a simple two dimensional mapping derived previously.⁽¹⁾ We found that the number of iteration necessary to converge within certain distance from the major attractor is inversely proportional to the amount of the dissipation.

§ 2. Mapping Model

To investigate the effect of weak dissipation on the drift orbit mapping, we consider the two dimensional mapping in the phase space (θ, x) derived previously⁽¹⁾:

$$\begin{aligned} x_{n+1} &= (1 - c_d) x_n + K \sin l\theta_n, \\ \theta_{n+1} &= \theta_n + \iota_0(1 - s x_{n+1}), \end{aligned} \quad (1)$$

where x is the normalized radial coordinate, θ is the poloidal angle, c_d is the dissipation due to resistivity in the generalized Ohm law, ι_0 is the rotational transform of the helical magnetic field, and K is proportional to the amplitude of the helical field. The mapping (1) is similar to the dissipative standard map⁽²⁾.

In the derivation of the mapping (1), we have assumed that the $E \times B$ drift and curvature drift replaced by the diamagnetic drift motions in the poloidal direction can be neglected, and the helical field amplitude is uniform with respect to the radius r which may be applicable to the $l=1$ helical field. For the $l=1$ helical field, however, the magnetic axis becomes a helix. The mapping (1) does not include this helical axis effect, and may be applicable for a small helical amplitude or in the region away from the axis. In spite of many approximations, the mapping (1) still should have essentially important characteristics such as basic orbit configuration and its transition to chaos.

Since c_d is very small, the period one fixed point of the map (1) is determined as

$$x = -1/s \quad \text{and} \quad \theta = 0. \quad (2)$$

The stability of the fixed point is determined by the eigenvalue λ of the tangent map for Eq. (1):

$$\lambda = 1 - 2R + 2(R(R-1))^{1/2}, \quad (3)$$

where R is the residue⁽³⁾ given by $R = (2 - \text{Tr}(T))/4 = (c_d - Ks\iota_0)/4$. The fixed point is stable when $0 < R < 1$. In this case the eigenvalue may be expressed by $\lambda = \exp(ip)$. From Eq.(3), the argument p is expressed by $\cos p = 1 + \iota_0 Ks/2$ or

$$p = \cos^{-1}(1 + \iota_0 Ks/2) \quad (4)$$

where the dissipation c_d has been neglected, because it has been assumed to be very small.

§ 3. Numerical Results

First we start with the area preserving map ($c_d=0$). The Poincare mapping of Eq.(1) for 64 orbits after 5000 iterations are presented in Fig.1 where last 500 points are plotted for the case of $K=0.3$, $\iota_0=2.123$, $s=-1$, and $c_d=0$. As in the typical area preserving case, the chaotic region is limited near the separatrix, which may be induced by interaction of small scale islands.

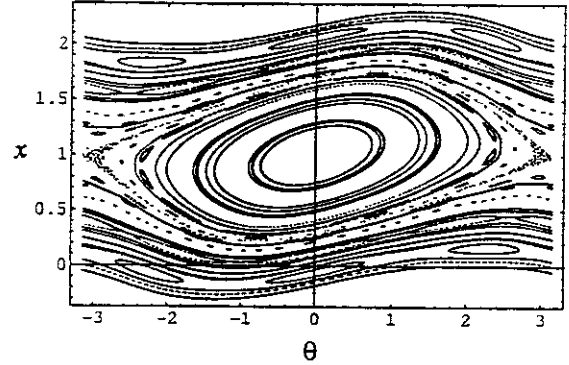


Fig.1: Poincaré mapping of orbits in Hamiltonian system

To investigate how these orbits may change with the dissipation, we introduced a weak dissipation ($c_d=0.0001$) in the system. Results for the same parameters and the same orbits as in the case in Fig. 1, is presented in Fig.2 where the iteration number $N=5000$, and the last 500 points are also plotted for each orbit.

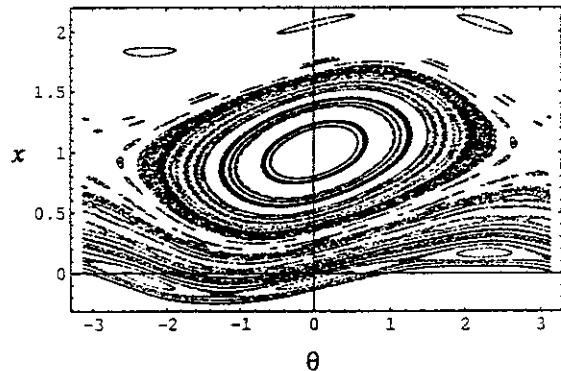


Fig.2: Poincaré mapping of orbits with small dissipation. As seen in Fig.2, with the small dissipation, each surface seems to have "thickness" and looks chaotic. It is not necessarily chaotic.⁽⁴⁾ Also we notice that the sizes of islands shrink. Increasing the number of iterations, each island shrinks and tends to the center of axis or the attractor, which can be seen in Fig.3 where N is increased to

50000. Each orbit converges to the center of near by island which can be considered as the attractor of the dissipative system. Increasing the number of iterations all orbits converge to the corresponding attractors. This also means that even an initially chaotic orbit near the separatrix is stabilized and converges to the attractor with a small dissipation. Since many orbits may converge to the limited area near the attractors after many iterations, and since the number of iterations means the number of toroidal circulations of the orbit, the plasma may be condensed and form filamentary shape in the final steady state.

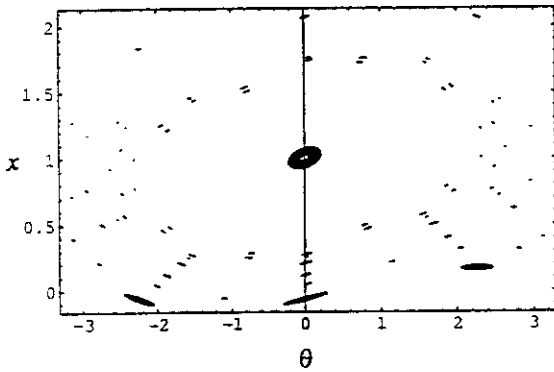


Fig.3: Poincare mapping after 50000 iterations

To see how these orbits converge to the attractor, we plot the last 2000 points with $N=8000$. As presented in Fig.4, the orbit forms vortex, the top of the each vortex

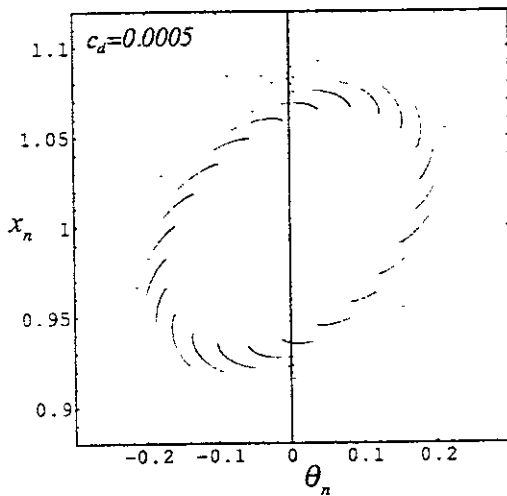


Fig.4. Convergence behavior of orbit near attractor

line converges rotating around the attractor as we increase the iteration number N . The number of vortex lines may depend on the rotation number at the attractor. The rotation angle ρ given by Eq.(4) in the case of Fig.4, i.e., $\nu_0=2.123$, $s=-1$ and $K=0.3$, is $\rho=0.821$ rad. If the orbit approximately closes by itself after m and n rotations in the poloidal and toroidal(axial) directions, respectively, we have $\rho/2\pi=m/n$, and find $m=3$ for $n=23$ as seen in Fig.4.

The convergence radius formed by the top of the vortex lines depend strictly on the iteration number N and also on the dissipation c_d . We calculated the convergent radii for various values of c_d and N . In Fig.5, the last 46 points of the x -coordinate are plotted as a function of the dissipation c_d for $N=3000$ and 5000 . We can see that for a fixed N , the convergence is faster for larger c_d .

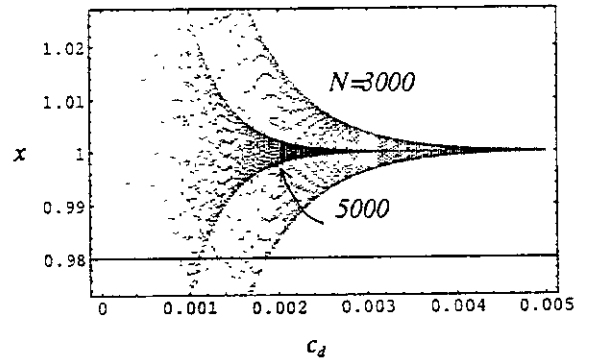


Fig.5 Variation of convergent radii versus c_d .

In order to see the convergence of these top of the vortex lines, the x -coordinate of the last 50-points are also plotted as a function of N in Fig. 6, where the comparison is also made for two different dissipations. One will see clearly in Fig.6 that the convergence is much faster for

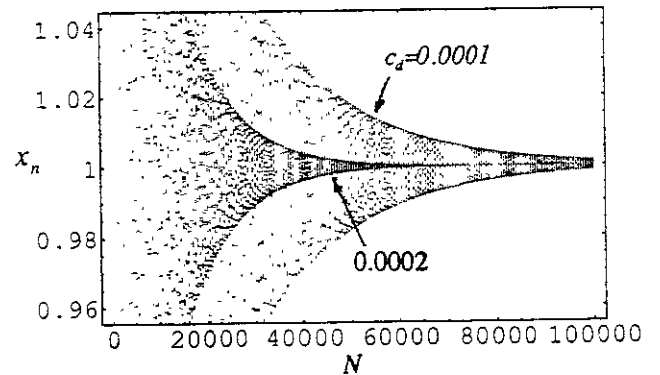


Fig.6 Convergent radii versus N for two values of c_d

larger dissipations. From Fig.6, we may obtain a rough scaling of the iteration number N versus c_d : Since the convergence radius r_c at $N=100000$ for the case of $c_d=0.0001$ is nearly the same as the radius r_c at $N=50000$ for the case of $c_d=0.0002$, we may, therefore, presume $N \cdot c_d \sim 10 = \text{constant}$, i.e., the number of iteration N is inversely proportional to c_d for the convergence to the same radius r_c , $N \sim 10/c_d$, which means that the convergence is faster for the larger dissipation. Without the dissipation, $c_d \rightarrow 0$, any orbit cannot tend to the attractor in the dissipative system in a finite number of iteration N , which is physically reasonable.

Since the convergence scaling is important, we calculated more precisely the convergence radius r_c as a function of the iteration number N and the dissipation c_d . To evaluate the convergence radius r_c , we first evaluated the center point (attractor coordinate) by averaging the top points of the vortex lines. The convergence radius is, then, evaluated as the minimum of the distances between the top points and the center coordinate. When we calculated the radius r_c by the single precision in a FORTRAN program, it tended to a finite value and never approached to zero due to the numerical truncation error. We employed, therefore, the double precision, and obtained the results as presented in Fig.7 for two different values of c_d .

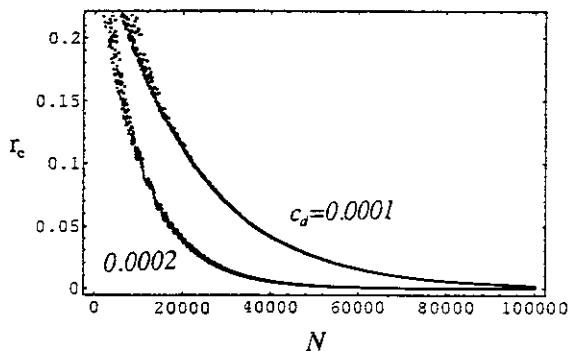


Fig.7: Variations of convergent radius versus N

To have the more accurate scaling, the number of iteration N to converge to a given radius r_c is calculated for various values of c_d , which are plotted versus c_d in logarithmic scales in Fig.8. As seen in Fig.8, the

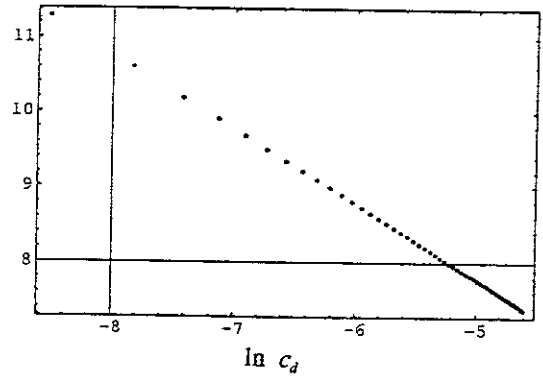


Fig.8: Variation of $\ln N$ versus $\ln c_d$ for $r_c=0.0001$.

variation of $\ln N$ is clearly linear with respect to $\ln c_d$, and can be expressed by $\ln N = 2.750 - 1.003 \ln c_d$ or $N = 15.64 c_d^{-1.003}$ which is close to the rough scaling obtained by the inspection in Fig. 6.

We now consider how many orbits starting from the various initial positions in the phase space converge to the area inside the radius r_c , πr_c^2 . The problem may be solved by evaluating the basin for the radius from the major attractor in the phase space. We evaluated the distance from the major attractor after N iterations for 300×300 orbits starting from the initial positions in the phase space, $0 < x < 2$, $-\pi < \theta < \pi$. Two dimensional graphics of the distance for $c_d = 0.0001$ and $N = 5000$ is presented in Fig.9, where the black portion means the distance is close to zero, while the white portion corresponds to a

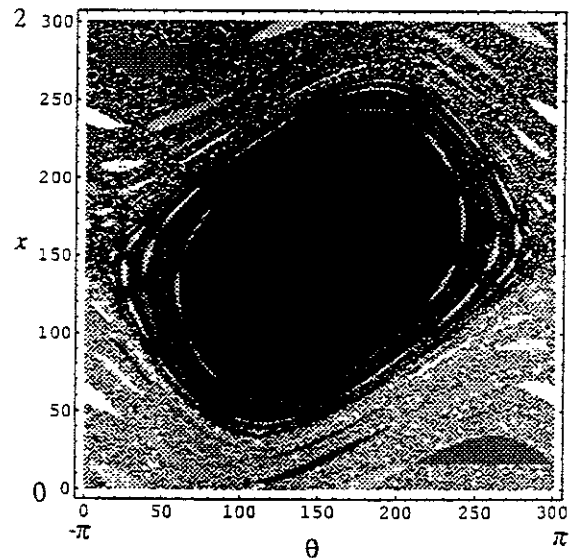


Fig.9: Two dimensional graphics of distance from attractor after 50000 iterations for $c_d=0.0001$

large distance from the major attractor. We see that almost all orbits except near the secondary islands inside the separatrix tend to the major attractor. In order to see more clearly the basin boundary for orbits which converge within radius r_a around the major attractor, we divided the set in Fig.9 into two group, the one with the distance from the attractor $d < r_a$ (black), and the other with $d > r_a$ (white). The result is plotted in Fig.10 for $r_a=0.2$. The orbits starting from black region should converge within the radius 0.2 from the attractor. We can see that many orbits even outside (upper portion) of the separatrix tend to the region near the attractor.

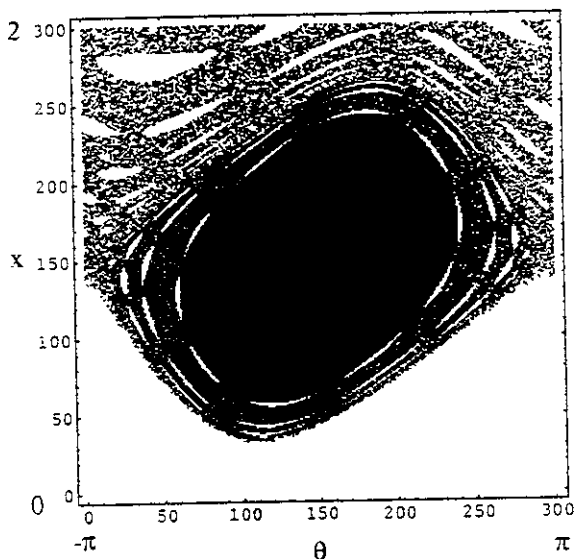


Fig.10: Basin of orbits which converge within $r_a=0.2$.

The white holes in Fig.10 may be considered as the secondary islands. The orbits inside these holes may converge to their own attractor (the center of the island). If we limit the convergent radius $r_a=0.05$, the basin changes as shown in Fig.11, i.e., the orbits starting from the black region converge within the distance 0.05 from the attractor after 50000 iterations. We can see fine scale holes also in Fig.11, which may be fine scale islands. As we have seen, the evaluation of the basin boundary is equivalent to solving the nonlinear initial value problem. As will be discussed in the next section, the width of the basin of the convergent orbits is very important for the

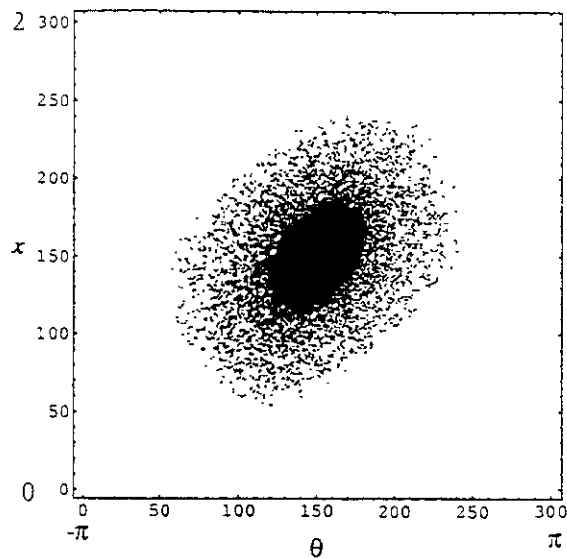


Fig.11: Basin for $r_a=0.05$ and $c_d=0.0001$.

evaluation of the compression ratio of a plasma density.

§ 4. Summary and Discussion

Making use of a simple mapping model for electron drift motion, we found that orbits obtained by the area preserving map are completely changed by a small amount of dissipation. Each orbit tends to the attractor forming vortex line encircling the attractor in the dissipative system. Although each orbit changes significantly, the basic characteristics (stability) of the mapping does not change, i.e., the stable fixed o-point or the island center does not change, because the amount of the dissipation introduced is very small. These stable fixed o-points in the area preserving system, therefore, become the attractors in the dissipative system. Any orbit starting from any point in the phase space converges to one of these attractors after many iterations. This means that initially uniformly distributed orbits may change to filamentary set of orbit around the attractors.

Mathematically, we have solved a nonlinear initial value problem for the two dimensional mapping with a very small dissipation by calculating the convergent radii and basin boundaries.

As presented in the previous section, particles within the

separatrix may be concentrated near the center (attractor) after N time circulating in the toroidal direction. If the area of basin is S_0 , and the concentrated area is $S_a = \pi r_a^2$, the initial particle density n_0 inside the basin may be increased by $R = S_0/S_a$ after N circulations. The time for one toroidal circuration is given by the transit time $\tau = 2\pi/(k_{\parallel} v)$, the time t_N necessary to concentrate to S_a is given by $t_N = 2\pi N/(k_{\parallel} v)$, where k_{\parallel} is the pararel wave number and v is the thermal velocity.

If we assume $c_a = 0.0001$, $S_0 = \pi$ (with the radius 1), $r_a = 0.5$, $N = 25000$ and $\tau = 1\text{MHz}$, then the concentration ratio becomes $R = 4$ and $t_N = 0.025$ s, i.e., the particle density may increase by a factor 4 in 0.025 s. This number N is reduced significantly by increasing the amount of the dissipation as presented in the previous section. This concentration of density may be considered as a pinch effect due to the nonlinear dissipation. The density peak observed away from the center in Stellarators⁽⁴⁾ might be related to this phenomenon.

The concentration of orbit due to the dissipation may be important for the edge plasmas because the effect of dissipation may be significant in the peripheral regions. Since the dissipation may be controlable to some extent from out side, we may controle the configuration of plasmas by changing the amount of the dissipation.

Although our mapping model may be too simple, the concentration of orbits with a small dissipation has also

been observed in numerical solutions of nonlinear differential equations⁽⁵⁾. The results obtained in our model, therefore, must be universal.

Construction of mapping equations in more realistic configurations, development of the mapping theory itself, and the relation between discrete mapping and the system of nonlinear differential equations are remained to be studied.

Acknowledgment

The author would like to thank to Prof. Ichikawa for his encouragement. This study is a joint research effort with the National Institute for Fusion Science. The most of numerical calculations were made using a Fujitsu VPP-500 in the computer center of Tokyo Metropolitan Institute of Technology.

References

- (1) T. Yamagishi; J. Plasma Fusion Research, SERIES 1(1998)507.
- (2) T. Bohr, P. Bak and M.H. Jensen; Phys. Rev. A, 30 (1984)1970.
- (3) J.M. Greene, J. Math. Phys. 20 (1969)1183.
- (4) H. Iguchi, K. Ida, H. Yamada, et al.; Report NIFS-267(1994).
- (5) T. Yamagishi and M. Tsukayama; Memoir of Tokyo Metro. Inst. Technol., 13(1999)49.

Recent Issues of NIFS Series

- NIFS-564 T. Watan, T. Shimozuma, Y. Takeiri, R. Kumazawa, T. Mutoh, M. Sato, O. Kaneko, K. Ohkubo, S. Kubo, H. Idei, Y. Oka, M. Osakabe, T. Seki, K. Tsumori, Y. Yoshimura, R. Akiyama, T. Kawamoto, S. Kobayashi, F. Shimpō, Y. Takita, E. Asano, S. Itoh, G. Nomura, T. Ido, M. Hamabe, M. Fujiwara, A. Iiyoshi, S. Morimoto, T. Bigelow and Y.P. Zhao,
Steady State Heating Technology Development for LHD; Oct 1998
(IAEA-CN-69/FTP/21)
- NIFS-565 A. Sagara, K.Y. Watanabe, K. Yamazaki, O. Motojima, M. Fujiwara, O. Mitarai, S. Imagawa, H. Yamanishi, H. Chikaraishi, A. Kohyama, H. Matsui, T. Muroga, T. Noda, N. Ohyabu, T. Satow, A.A. Shishkin, S. Tanaka, T. Tera and T. Uda,
LHD-Type Compact Helical Reactors; Oct 1998
(IAEA-CN-69/FTP/03(R))
- NIFS-566 N. Nakajima, J. Chen, K. Ichiguchi and M. Okamoto,
Global Mode Analysis of Ideal MHD Modes in L=2 Heliotron/Torsatron Systems; Oct. 1998
(IAEA-CN-69/THP1/08)
- NIFS-567 K. Ida, M. Osakabe, K. Tanaka, T. Minami, S. Nishimura, S. Okamura, A. Fujisawa, Y. Yoshimura, S. Kubo, R. Akiyama, D.S. Darrow, H. Idei, H. Iguchi, M. Isobe, S. Kado, T. Kondo, S. Lee, K. Matsuoka, S. Morita, I. Nomura, S. Ohdachi, M. Sasao, A. Shimizu, K. Tsumori, S. Takayama, M. Takechi, S. Takagi, C. Takahashi, K. Toi and T. Watan,
Transition from L Mode to High Ion Temperature Mode in CHS Heliotron/Torsatron Plasmas; Oct 1998
(IAEA-CN-69/EX2/2)
- NIFS-568 S. Okamura, K. Matsuoka, R. Akiyama, D.S. Darrow, A. Ejiri, A. Fujisawa, M. Fujiwara, M. Goto, K. Ida, H. Idei, H. Iguchi, N. Inoue, M. Isobe, K. Itoh, S. Kado, K. Khlopenkov, T. Kondo, S. Kubo, A. Lazaros, S. Lee, G. Matsunaga, T. Minami, S. Morita, S. Murakami, N. Nakajima, N. Nikai, S. Nishimura, I. Nomura, S. Ohdachi, K. Ohkuni, M. Osakabe, R. Pavlichenko, B. Peterson, R. Sakamoto, H. Sanuki, M. Sasao, A. Shimizu, Y. Shirai, S. Sudo, S. Takagi, C. Takahashi, S. Takayama, M. Takechi, K. Tanaka, K. Toi, K. Yamazaki, Y. Yoshimura and T. Watan,
Confinement Physics Study in a Small Low-Aspect-Ratio Helical Device CHS; Oct 1998
(IAEA-CN-69/OV4/5)
- NIFS-569 M.M. Skonc, T. Sato, A. Maluckov, M.S. Jovanovic,
Micro- and Macro-scale Self-organization in a Dissipative Plasma; Oct 1998
- NIFS-570 T. Hayashi, N. Mizuguchi, T.H. Watanabe, T. Sato and the Complexity Simulation Group,
Nonlinear Simulations of Internal Reconnection Event in Spherical Tokamak; Oct 1998
(IAEA-CN-69/TH3/3)
- NIFS-571 A. Iiyoshi, A. Komori, A. Ejiri, M. Emoto, H. Funaba, M. Goto, K. Ida, H. Idei, S. Inagaki, S. Kado, O. Kaneko, K. Kawahata, S. Kubo, R. Kumazawa, S. Masuzaki, T. Minami, J. Miyazawa, T. Morisaki, S. Morita, S. Murakami, S. Muto, T. Muto, Y. Nagayama, Y. Nakamura, H. Nakanishi, K. Narihara, K. Nishimura, N. Noda, T. Kobuchi, S. Ohdachi, N. Ohyabu, Y. Oka, M. Osakabe, T. Ozaki, B.J. Peterson, A. Sagara, S. Sakakibara, R. Sakamoto, H. Sasao, M. Sasao, K. Sato, M. Sato, T. Seki, T. Shimozuma, M. Shoji, H. Suzuki, Y. Takeiri, K. Tanaka, K. Toi, T. Tokuzawa, K. Tsumori, I. Yamada, H. Yamada, S. Yamaguchi, M. Yokoyama, K.Y. Watanabe, T. Watan, R. Akiyama, H. Chikaraishi, K. Haba, S. Hamaguchi, S. Ima, S. Imagawa, N. Inoue, K. Iwamoto, S. Kitagawa, Y. Kubota, J. Kodaira, R. Maekawa, T. Mito, T. Nagasaka, A. Nishimura, Y. Takita, C. Takahashi, K. Takahata, K. Yamauchi, H. Tamura, T. Tsuzuki, S. Yamada, N. Yanagi, H. Yonezu, Y. Hamada, K. Matsuoka, K. Murai, K. Ohkubo, I. Ohtake, M. Okamoto, S. Sato, T. Satow, S. Sudo, S. Tanahashi, K. Yamazaki, M. Fujiwara and O. Motojima,
An Overview of the Large Helical Device Project; Oct. 1998
(IAEA-CN-69/OV1/4)
- NIFS-572 M. Fujiwara, H. Yamada, A. Ejiri, M. Emoto, H. Funaba, M. Goto, K. Ida, H. Idei, S. Inagaki, S. Kado, O. Kaneko, K. Kawahata, A. Komori, S. Kubo, R. Kumazawa, S. Masuzaki, T. Minami, J. Miyazawa, T. Morisaki, S. Morita, S. Murakami, S. Muto, T. Muto, Y. Nagayama, Y. Nakamura, H. Nakanishi, K. Narihara, K. Nishimura, N. Noda, T. Kobuchi, S. Ohdachi, N. Ohyabu, Y. Oka, M. Osakabe, T. Ozaki, B. J. Peterson, A. Sagara, S. Sakakibara, R. Sakamoto, H. Sasao, M. Sasao, K. Sato, M. Sato, T. Seki, T. Shimozuma, M. Shoji, H. Suzuki, Y. Takeiri, K. Tanaka, K. Toi, T. Tokuzawa, K. Tsumori, I. Yamada, S. Yamaguchi, M. Yokoyama, K.Y. Watanabe, T. Watan, R. Akiyama, H. Chikaraishi, K. Haba, S. Hamaguchi, M. Ima, S. Imagawa, N. Inoue, K. Iwamoto, S. Kitagawa, Y. Kubota, J. Kodaira, R. Maekawa, T. Mito, T. Nagasaka, A. Nishimura, Y. Takita, C. Takahashi, K. Takahata, K. Yamauchi, H. Tamura, T. Tsuzuki, S. Yamada, N. Yanagi, H. Yonezu, Y. Hamada, K. Matsuoka, K. Murai, K. Ohkubo, I. Ohtake, M. Okamoto, S. Sato, T. Satow, S. Sudo, S. Tanahashi, K. Yamazaki, O. Motojima and A. Iiyoshi,
Plasma Confinement Studies in LHD; Oct. 1998
(IAEA-CN-69/EX2/3)
- NIFS-573 O. Motojima, K. Akaishi, H. Chikaraishi, H. Funaba, S. Hamaguchi, S. Imagawa, S. Inagaki, N. Inoue, A. Iwamoto, S. Kitagawa, A. Komori, Y. Kubota, R. Maekawa, S. Masuzaki, T. Mito, J. Miyazawa, T. Morisaki, T. Muroga, T. Nagasaka, Y. Nakamura, A. Nishimura, K. Nishimura, N. Noda, N. Ohyabu, S. Sagara, S. Sakakibara, R. Sakamoto, S. Satoh, T. Satow, M. Shoji, H. Suzuki, K. Takahata, H. Tamura, K. Watanabe, H. Yamada, S. Yamada, S. Yamaguchi, K. Yamazaki, N. Yanagi, T. Baba, H. Hayashi, M. Ima, T. Inoue, S. Kato, T. Kato, T. Kondo, S. Moriuchi, H. Ogawa, I. Ohtake, K. Ooba, H. Sekiguchi, N. Suzuki, S. Takami, Y. Taniguchi, T. Tsuzuki, N. Yamamoto, K. Yasui, H. Yonezu, M. Fujiwara and A. Iiyoshi,
Progress Summary of LHD Engineering Design and Construction; Oct 1998
(IAEA-CN-69/FT2/1)
- NIFS-574 K. Toi, M. Takechi, S. Takagi, G. Matsunaga, M. Isobe, T. Kondo, M. Sasao, D.S. Darrow, K. Ohkuni, S. Ohdachi, R. Akiyama, A. Fujisawa, M. Gotoh, H. Idei, K. Ida, H. Iguchi, S. Kado, M. Kojima, S. Kubo, S. Lee, K. Matsuoka, T. Minami, S. Morita, N. Nikai,

- S. Nishimura, S. Okamura, M. Osakabe, A. Shimizu, Y. Shirai, C. Takahashi, K. Tanaka, T. Watari and Y. Yoshimura,
Global MHD Modes Excited by Energetic Ions in Heliotron/Torsatron Plasmas; Oct. 1998
(IAEA-CN-69/EXP1/19)
- NIFS-575 Y. Hamada, A. Nishizawa, Y. Kawasumi, A. Fujisawa, M. Kojima, K. Narihara, K. Ida, A. Ejiri, S. Ohdachi, K. Kawahata, K. Toi, K. Sato, T. Seki, H. Iguchi, K. Adachi, S. Hidekuma, S. Hirokura, K. Iwasaki, T. Ido, R. Kumazawa, H. Kuramoto, T. Minami, L. Nomura, M. Sasao, K.N. Sato, T. Tsuzuki, I. Yamada and T. Watari,
Potential Turbulence in Tokamak Plasmas; Oct. 1998
(IAEA-CN-69/EXP2/14)
- NIFS-576 S. Murakami, U. Gasparino, H. Idei, S. Kubo, H. Maassberg, N. Marushchenko, N. Nakajima, M. Romé and M. Okamoto,
5D Simulation Study of Suprathermal Electron Transport in Non-Axisymmetric Plasmas; Oct. 1998
(IAEA-CN-69/THP1/01)
- NIFS-577 S. Fujiwara and T. Sato,
Molecular Dynamics Simulation of Structure Formation of Short Chain Molecules; Nov. 1998
- NIFS-578 T. Yamagishi,
Eigenfunctions for Vlasov Equation in Multi-species Plasmas Nov. 1998
- NIFS-579 M. Tanaka, A. Yu Grosberg and T. Tanaka,
Molecular Dynamics of Strongly-Coupled Multichain Coulomb Polymers in Pure and Salt Aqueous Solutions; Nov. 1998
- NIFS-580 J. Chen, N. Nakajima and M. Okamoto,
Global Mode Analysis of Ideal MHD Modes in a Heliotron/Torsatron System: I. Mercier-unstable Equilibria; Dec. 1998
- NIFS-581 M. Tanaka, A. Yu Grosberg and T. Tanaka,
Comparison of Multichain Coulomb Polymers in Isolated and Periodic Systems: Molecular Dynamics Study; Jan. 1999
- NIFS-582 V.S. Chan and S. Murakami,
Self-Consistent Electric Field Effect on Electron Transport of ECH Plasmas; Feb. 1999
- NIFS-583 M. Yokoyama, N. Nakajima, M. Okamoto, Y. Nakamura and M. Wakatani,
Roles of Bumpy Field on Collisionless Particle Confinement in Helical-Axis Heliotrons; Feb. 1999
- NIFS-584 T.-H. Watanabe, T. Hayashi, T. Sato, M. Yamada and H. Ji,
Modeling of Magnetic Island Formation in Magnetic Reconnection Experiment; Feb. 1999
- NIFS-585 R. Kumazawa, T. Mutoh, T. Seki, F. Shinpo, G. Nomura, T. Ido, T. Watan, Jean-Marie Noterdaeme and Yangping Zhao,
Liquid Stub Tuner for Ion Cyclotron Heating; Mar. 1999
- NIFS-586 A. Sagara, M. Iima, S. Inagaki, N. Inoue, H. Suzuki, K. Tsuzuki, S. Masuzaki, J. Miyazawa, S. Morita, Y. Nakamura, N. Noda, B. Peterson, S. Sakakibara, T. Shimoizuma, H. Yamada, K. Akaishi, H. Chikaraishi, H. Funaba, O. Kaneko, K. Kawahata, A. Komori, N. Ohyabu, O. Motojima, LHD Exp. Group 1, LHD Exp. Group 2,
Wall Conditioning at the Starting Phase of LHD; Mar. 1999
- NIFS-587 T. Nakamura and T. Yabe,
Cubic Interpolated Propagation Scheme for Solving the Hyper-Dimensional Vlasov-Poisson Equation in Phase Space; Mar. 1999
- NIFS-588 W.X. Wnag, N. Nakajima, S. Murakami and M. Okamoto,
An Accurate δf Method for Neoclassical Transport Calculation; Mar. 1999
- NIFS-589 K. Kishida, K. Araki, S. Kishiba and K. Suzuki,
Local or Nonlocal? Orthonormal Divergence-free Wavelet Analysis of Nonlinear Interactions in Turbulence; Mar. 1999
- NIFS-590 K. Araki, K. Suzuki, K. Kishida and S. Kishiba,
Multiresolution Approximation of the Vector Fields on T^3 ; Mar. 1999
- NIFS-591 K. Yamazaki, H. Yamada, K.Y. Watanabe, K. Nishimura, S. Yamaguchi, H. Nakanishi, A. Komori, H. Suzuki, T. Mito, H. Chikaraishi, K. Murai, O. Motojima and the LHD Group,
Overview of the Large Helical Device (LHD) Control System and Its First Operation; Apr. 1999

- NIFS-592 T Takahashi and Y Nakao,
Thermonuclear Reactivity of D-T Fusion Plasma with Spin-Polarized Fuel, Apr 1999
- NIFS-593 H Sugama,
Damping of Toroidal Ion Temperature Gradient Modes, Apr 1999
- NIFS-594 Xiaodong Li,
Analysis of Crowbar Action of High Voltage DC Power Supply in the LHD ICRF System, Apr 1999
- NIFS-595 K Nishimura, R Honuchi and T Sato,
Drift-kink Instability Induced by Beam Ions in Field-reversed Configurations, Apr. 1999
- NIFS-596 Y Suzuki, T-H Watanabe, T Sato and T Hayashi,
Three-dimensional Simulation Study of Compact Toroid Plasmoid Injection into Magnetized Plasmas;
Apr 1999
- NIFS-597 H Sanuki, K Itoh, M Yokoyama, A Fujisawa, K Ida, S. Toda, S-i Itoh, M. Yagi and A Fukuyama,
Possibility of Internal Transport Barrier Formation and Electric Field Bifurcation in LHD Plasma;
May 1999
- NIFS-598 S. Nakazawa, N Nakajima, M. Okamoto and N. Ohyabu,
One Dimensional Simulation on Stability of Detached Plasma in a Tokamak Divertor, June 1999
- NIFS-599 S. Murakami, N. Nakajima, M. Okamoto and J. Nhrenberg,
Effect of Energetic Ion Loss on ICRF Heating Efficiency and Energy Confinement Time in Heliotrons,
June 1999
- NIFS-600 R. Honuchi and T. Sato,
Three-Dimensional Particle Simulation of Plasma Instabilities and Collisionless Reconnection in a Current Sheet, June 1999
- NIFS-601 W. Wang, M. Okamoto, N. Nakajima and S. Murakami,
Collisional Transport in a Plasma with Steep Gradients, June 1999
- NIFS-602 T. Mutoh, R. Kumazawa, T. Saki, K. Saito, F. Simpo, G. Nomura, T. Watan, X. Jikang, G. Cattanei, H. Okada, K. Ohkubo, M. Sato, S. Kubo, T. Shimozuma, H. Idei, Y. Yoshimura, O. Kaneko, Y. Takeiri, M. Osakabe, Y. Oka, K. Tsumori, A. Komori, H. Yamada, K. Watanabe, S. Sakakibara, M. Shoji, R. Sakamoto, S. Inagaki, J. Miyazawa, S. Monta, K. Tanaka, B.J. Peterson, S. Murakami, T. Minami, S. Ohdachi, S. Kado, K. Narihara, H. Sasao, H. Suzuki, K. Kawahata, N. Ohyabu, Y. Nakamura, H. Funaba, S. Masuzaki, S. Muto, K. Sato, T. Monsaki, S. Sudo, Y. Nagayama, T. Watanabe, M. Sasao, K. Ida, N. Noda, K. Yamazaki, K. Akaishi, A. Sagara, K. Nishimura, T. Ozaki, K. Toi, O. Motojima, M. Fujiwara, A. Iiyoshi and LHD Exp. Group 1 and 2,
First ICRF Heating Experiment in the Large Helical Device, July 1999
- NIFS-603 P.C. de Vries, Y. Nagayama, K. Kawahata, S. Inagaki, H. Sasao and K. Nagasaki,
Polarization of Electron Cyclotron Emission Spectra in LHD; July 1999
- NIFS-604 W. Wang, N. Nakajima, M. Okamoto and S. Murakami,
 δf Simulation of Ion Neoclassical Transport; July 1999
- NIFS-605 T. Hayashi, N. Mizuguchi, T. Sato and the Complexity Simulation Group,
Numerical Simulation of Internal Reconnection Event in Spherical Tokamak, July 1999
- NIFS-606 M. Okamoto, N. Nakajima and W. Wang,
On the Two Weighting Scheme for δf Collisional Transport Simulation, Aug 1999
- NIFS-607 O. Motojima, A.A. Shishkin, S. Inagaki, K.Y. Watanabe,
Possible Control Scenario of Radial Electric Field by Loss-Cone-Particle Injection into Helical Device, Aug 1999
- NIFS-608 R. Tanaka, T. Nakamura and T. Yabe,
Constructing Exactly Conservative Scheme in Non-conservative Form, Aug 1999
- NIFS-609 H Sugama,
Gyrokinetic Field Theory, Aug. 1999
- NIFS-610 M. Takechi, G. Matsunaga, S. Takagi, K. Ohkuni, K. Toi, M. Osakabe, M. Isobe, S. Okamura, K. Matsuoka, A. Fujisawa, H. Iguchi, S. Lee, T. Minami, K. Tanaka, Y. Yoshimura and CHS Group,

Core Localized Toroidal Alfvén Eigenmodes Destabilized By Energetic Ions in the CHS Heliotron/Torsatron; Sep. 1999

- NIFS-611 K Ichiguchi,
MHD Equilibrium and Stability in Heliotron Plasmas; Sep. 1999
- NIFS-612 Y. Sato, M. Yokoyama, M. Wakatani and V. D. Pusovitch,
Complete Suppression of Pfirsch-Schluter Current in a Toroidal $l=3$ Stellarator; Oct. 1999
- NIFS-613 S. Wang, H. Sanuki and H. Sugama,
Reduced Drift Kinetic Equation for Neoclassical Transport of Helical Plasmas in Ultra-low Collisionality Regime; Oct. 1999
- NIFS-614 J. Miyazawa, H. Yamada, K. Yasui, S. Kato, N., Fukumoto, M. Nagata and T. Uyama,
Design of Spheromak Injector Using Conical Accelerator for Large Helical Device, Nov 1999
- NIFS-615 M. Uchida, A. Fukuyama, K. Itoh, S.-I. Itoh and M. Yagi,
Analysis of Current Diffusive Ballooning Mode in Tokamaks; Dec. 1999
- NIFS-616 M. Tanaka, A.Yu Grosberg and T. Tanaka,
Condensation and Swelling Behavior of Randomly Charged Multichain Polymers by Molecular Dynamics Simulations; Dec. 1999
- NIFS-617 S. Goto and S. Kida,
Sparseness of Nonlinear Coupling; Dec. 1999
- NIFS-618 M.M. Skoric, T. Sato, A. Maluckov and M.S. Jovanovic,
Complexity in Laser Plasma Instabilities Dec. 1999
- NIFS-619 T.-H. Watanabe, H. Sugama and T. Sato,
Non-dissipative Kinetic Simulation and Analytical Solution of Three-mode Equations of Ion Temperature Gradient Instability; Dec. 1999
- NIFS-620 Y. Oka, Y. Takeiri, Yu.I. Belchenko, M. Hamabe, O. Kaneko, K. Tsumori, M. Osakabe, E. Asano, T. Kawamoto, R. Akiyama,
Optimization of Cs Deposition in the 1/3 Scale Hydrogen Negative Ion Source for LHD-NBI System ;Dec. 1999
- NIFS-621 Yu.I. Belchenko, Y. Oka, O. Kaneko, Y. Takeiri, A. Krivenko, M. Osakabe, K. Tsumori, E. Asano, T. Kawamoto, R. Akiyama,
Recovery of Cesium in the Hydrogen Negative Ion Sources; Dec. 1999
- NIFS-622 Y. Oka, O. Kaneko, K. Tsumori, Y. Takeiri, M. Osakabe, T. Kawamoto, E. Asano, and R. Akiyama,
H- Ion Source Using a Localized Virtual Magnetic Filter in the Plasma Electrode: Type I LV Magnetic Filter: Dec. 1999
- NIFS-623 M. Tanaka, S. Kida, S. Yanase and G. Kawahara,
Zero-absolute-vorticity State in a Rotating Turbulent Shear Flow; Jan. 2000
- NIFS-624 F. Leuterer, S. Kubo,
Electron Cyclotron Current Drive at $\omega \approx \omega_c$ with X-mode Launched from the Low Field Side; Feb 2000
- NIFS-625 K. Nishimura,
Wakefield of a Charged Particulate Influenced by Emission Process of Secondary Electrons; Mar. 2000
- NIFS-626 K. Itoh, M. Yagi, S.-I. Itoh, A. Fukuyama,
On Turbulent Transport in Burning Plasmas; Mar. 2000
- NIFS-627 K. Itoh, S.-I. Itoh, L. Giannone,
Modelling of Density Limit Phenomena in Toroidal Helical Plasmas; Mar. 2000
- NIFS-628 K. Akaishi, M. Nakasuga and Y. Funato,
True and Measured Outgassing Rates of a Vacuum Chamber with a Reversibly Absorbed Phase; Mar. 2000
- IFS-629 T. Yamagishi,
Effect of Weak Dissipation on a Drift Orbit Mapping; Mar. 2000